Journal of *Marine Science and Engineering*

MDPI

Article

Characteristics of Chromophoric Dissolved Organic Matter (CDOM) Produced by Heterotrophic Bacteria Isolated from Aquaculture Systems

Mariel Gullian-Klanian [1], Gerardo Gold-Bouchot [2,*] and María José Sánchez-Solís [1]

[1] School of Natural Resources, University Marist of Merida, Periférico Nte Tablaje Catastral 13941, Merida 97300, Mexico; mgullian@marista.edu.mx (M.G.-K.); msanchez@marista.edu.mx (M.J.S.-S.)
[2] Department of Oceanography and Geochemical and Environmental Research Group (GERG), Texas A&M University, College Station, TX 77843, USA
* Correspondence: ggold@tamu.edu

Abstract: Heterotrophic bacteria (HB) play an important role in aquatic ecosystems as recyclers of dissolved organic matter (DOM). The objective of this study was to characterize the spectral characteristics of intracellular (IC), and extracellular (EC) compounds produced by 12 HB isolated from two aquaculture systems. Microorganisms belonging to the genera *Bacillus*, *Paenibacillus*, and *Psychrobacillus* were identified by analysis of the 16S ribosomal gene. Aliquots of bacterial culture were centrifugated every hour (1st to 7th) to obtain the EC compounds. The pellet was ultrasound-lysed to obtain the IC compounds. Excitation-emission matrices were used in combination with parallel factor analysis (PARAFAC) to characterize the fluorescent components of DOM (FDOM). PARAFAC indicated two protein-like components and two humic-like components in both cell spaces. At the IC, *B. macquariensis* showed a high fluorescence index (FI), probably associated with fulvic acid, quinones, or ketones. *Psychrobacillus insolitus* showed an inverse correlation between spectral slopes $S_{275–295}$ and $S_{350–400}$ in the EC and IC fractions, which may indicate differential release of low and high molecular weight molecules in these two fractions. The opposite occurred with *B. licheniformis* and *P. alvei*. The origin of FDOM in HB is an important finding of this work. The most significant amount of protein-like substances was produced at the IC level, with the humic- and fulvic-type at the EC. The main finding of this work is the evidence of differential production of humic-type or protein-type FDOM production by HB species from marine and freshwater aquaculture systems in their intracellular and extracellular fractions, as well different relative molecular weight. For aquaculture, these findings suggest that some bacterial species show promise in supplying essential amino acids to growing organisms, and others play a major role in nutrient exchange and the global carbon cycle.

Keywords: FDOM; *Bacillus*; *Paenibacillus*; *Psychrobacillus*; PARAFAC

check for updates

Citation: Gullian-Klanian, M.; Gold-Bouchot, G.; Sánchez-Solís, M.J. Characteristics of Chromophoric Dissolved Organic Matter (CDOM) Produced by Heterotrophic Bacteria Isolated from Aquaculture Systems. *J. Mar. Sci. Eng.* **2022**, *10*, 672. https://doi.org/10.3390/jmse10050672

Academic Editor: Daniel M. Alongi

Received: 17 March 2022
Accepted: 10 May 2022
Published: 14 May 2022

Publisher's Note: MDPI stays neutral with regard to jurisdictional claims in published maps and institutional affiliations.

Copyright: © 2022 by the authors. Licensee MDPI, Basel, Switzerland. This article is an open access article distributed under the terms and conditions of the Creative Commons Attribution (CC BY) license (https://creativecommons.org/licenses/by/4.0/).

1. Introduction

Heterotrophic bacteria (HB) play an important role in aquatic environments as recyclers of dissolved organic matter (DOM) [1]. HB generally release DOM as metabolic by-products or because of the uncoupling of catabolic and anabolic processes [2]. They also actively release organic compounds for different cellular processes such as siderophores for iron absorption [3], acylated homoserine lactones for quorum detection [4], or polymers for enzymatic cleavage [5]. The Bacillus class consists of the most taxonomically diverse bacterial genera of the phylum Firmicutes. The class includes the Bacillaceae family, characterized by rod-shaped HB with the ability to form endospores, and the Paenibacillaceae family, a relatively new taxonomic classification containing the genus *Paenibacillus* [6]. The released products may differ between the different taxa [7,8] or change depending on environmental variables and nutrient concentrations [9,10].

HB have relevant roles in the carbon-nitrogen cycle in aquaculture production systems. They intervene in the availability of nutrients, the improvement of water quality, and the control of diseases and nutrition. Some aquaculture technologies, such as biofloc and suspended sludge production [11,12], promote mass production of HB in the water column to reduce production costs [13]. In addition to controlling toxic ammonia in the water, the heterotrophic microbiota represents an essential complementary food source for growing fish and crustaceans [14,15].

DOM is the main substrate for heterotrophic respiration and microbial growth [16]. Chromophoric dissolved organic matter (CDOM) is the chromophoric part of dissolved organic matter that absorbs light in the ultraviolet and visible (UV-Vis) wavelength range. The light emission and absorption properties of CDOM can affect the primary productivity in the water column and, therefore, water quality [17]. Fluorescent DOM (FDOM) is the fraction of CDOM capable of emitting fluorescence [18,19]. Variations in the fluorescence characteristics of CDOM have been associated with changes in bacterial metabolism [20–23]. Currently, very little is known about the characteristics of FDOM produced by marine individual heterotrophic species.

Bacterial phylogenetic groups differ in their dissolved organic components, mainly because their metabolic systems are different [22,24]. All microorganisms produce natural intracellular (IC) and extracellular (EC) fluorophores, whose concentrations depend on the physiological state of the cells [23,25]. Many biomolecules, including proteins, enzymes, coenzymes, pigments, and primary or secondary metabolites (e.g., fulvic and humic acids), exhibit characteristic fluorescence [26,27]. Fluorescence excitation-emission spectroscopy (EEM) matrices, together with parallel factor analysis (PARAFAC), have been used to characterize organic matter in natural aquatic systems and in vitro bacterial cultures, mainly due to the high selectivity and sensitivity [22,28,29]. According to EEM spectroscopy, the optically active fraction of FDOM has two main contributions: one similar to proteins (λex/λem 230–280/330–360 nm), and the other similar to humic and fulvic compounds [18,30]. Both contributions have been routinely divided into several subdivisions: tyrosine, tryptophan, and phenylalanine-like fluorescence for protein-like FDOM, visible and UV-like for humic-like FDOM [18,31]. PARAFAC enables the mathematical separation of overlapping chemically independent fluorescence components and their relative contributions to the EEMs [32,33].

Although there is knowledge about the production of FDOM in aquatic microbial communities, there is very little evidence of the production of humic-like or protein-like FDOM of HB from aquaculture environments. Hamby et al. [34] first used the EEM to characterize organic matter in a recirculating aquaculture system. Their results showed a 5-component PARAFAC model to describe organic matter of a recirculating aquaculture system. In our previous work, we studied the effect of incorporating *Bacillus* spp. on the characteristics of FDOM and mineralization in a recirculating aquaponic system [35]. Fox et al. [25] developed a methodology to study human pathogenic bacteria's intracellular and extracellular FDOM production. Goto et al. [36,37] described FDOM produced by *Alteromonas macleodii* and *Vibrio superbus* and *Phaeobacter gallaeciencis* in cultures with glucose as the only carbon source. In the present study, we focus on studying the intracellular and extracellular origin of FDOM in some heterotrophic species of aquaculture origin. Some species of the genera *Bacillus* and *Paenibacillus* are characterized as having an important environmental role as recyclers of organic material and are used to develop sustainable production technologies [35]. This is an in vitro study where each species was grown individually, which avoids the complexities of interpretation that microbial communities represent. This work provides useful information to understand the role of HB in the biochemical cycle of dissolved organic matter in aquaculture environment.

2. Materials and Methods

2.1. Isolation of Bacteria

The bacteria were isolated from two commercial aquaculture systems in the last week of growth: the first from an outdoor sea cucumber production system (*Isostichopus badionotus*) exposed to environmental conditions, and the second from an indoor production of freshwater fish (*Oreochromis niloticus*). In the last weeks of growth, the density of suspended solids is more stable; the bacterial population is resident and wholly adapted to the water conditions. Forty-eight hours before harvest, the organisms do not feed, which implies a lower population of food-borne bacteria in the water.

The samples were obtained from the biofilm adhered to the walls of the seawater pond (SW) and from the biofloc suspended in the freshwater tanks (FW). Four species of *Bacillus* were isolated from the SW system and eight species from the FW system. The isolated species were purified up to the third generation. The phenotypic characterization of the isolates was carried out according to the guidelines of the Archaea and Bergey Bacteria Systematics Manual [38].

2.2. Amplification of the 16S Ribosomal RNA Gene and Phenotypic Characterization

Genomic DNA was obtained by protein lysis and digestion according to the method described by Altschul et al. [39]. The 16S ribosomal RNA gene was amplified by PCR using the universal primers 27f (5′-AGA GTT TGA TCM TGG CTC AG-3′) [40] and 1492r (5′-ACG GYT ACC TTG TTA CG-3′) [41]. The PCR reaction mix (25 µL) consisted of 10 mM Tris-HCl (pH 9.0), 50 mM KCl, 0.1% Triton X-100, 2.1 mM $MgCl_2$, 0.2 µM of each one of deoxynucleoside triphosphate (dNTP), 0.4 µM primer concentration, 50 ng of bacterial DNA, and 1 U of Taq DNA polymerase (Promega Corp., Madison, WI, USA). The amplification protocol was as follows: 1 cycle of 240 s at 94 °C, 40 cycles of 5 s at 94 °C, 45 s at 46 °C, and 90 s at 72 °C; there was a final cycle of 10 min at 72 °C. The PCR products were electrophoresed on a 2% agarose gel at 85 V.

The purified PCR products were sequenced by the Sanger method (Applied Biosystems 3730xl; Thermo-Fisher Scientific, Waltham, MA, USA) on an automated DNA sequencing analyzer. The sequences were analyzed using the basic local alignment search tool (BLAST) [41]. The sequences were aligned with CLUSTAL W. The identity of the strains was determined by comparing the sequences with the NCBI-16S rRNA database.

2.3. Bacterial Growth Curves

Norris nitrogen-free and sodium citrate modified medium was used as the basal medium for microbial growth [42]. The formulation included 1.0% $C_6H_{12}O_6$, 0.08% $Na_3C_6H_5O_7$, 0.1% K_2HPO_4, 0.1% $CaCO_3$, 0.02% $MgSO_4$, 0.02% NaCl, 0.01% $FeSO_4$, and 0.001% Na_2MoO_4, (pH = 7.0 ± 0.2). NaCl (up to 1.5%) was added to the final formulation of the marine species. The sterilization of the culture medium and the experimental test material was carried out in a steam autoclave at 121 °C (FE-396—Felisa, Jalisco, MX, USA).

The cryopreserved bacteria were spread on tryptic soy agar (TSA, Difco 236950) and subsequently on Bacillus agar (PEMBA, Neogene NCM016) and incubated both times overnight at 28 °C. Growth curves were made by inoculating a single colony into 50 mL of modified Norris broth. The flask was incubated overnight at 28 °C (16 h) and shaken at 150 rpm (Barnstead MaxQ 4000 Orbital, Thermo-Fisher Scientific, Waltham, MA, USA). Subsequently, each culture was diluted in 150 mL of sterile Norris broth and incubated under the same conditions described above. After that, a 100 mL aliquot was suspended in a new flask with 200 mL of fresh Norris broth. The study was carried out during 7 h of the exponential phase to record the highest cellular activity. Once the absorbance reached the optical density (OD) of 0.02 (time 0), 25 mL were withdrawn from the culture and used for the cell count and the separation of the IC and EC components. OD was measured at a wavelength of 600 nm in a visible light spectrophotometer (Spectronic Genesys 20—Thermo-Fisher Scientific, Waltham, MA, USA). Norris's medium was used as a blank. Bacteria counting was performed using the Neubauer cell counting chamber. Samples were

diluted 1/200 in 2.5% glutaraldehyde and viewed under a phase-contrast microscope at 100× magnification.

2.4. Separation of Extracellular (EC) and Intracellular (IC) Bacterial Compounds

The separation of IC and EC components was carried out following the methodology described by Fox et al. [25] with some modifications. Bacterial culture samples were taken every hour in duplicate from the first hour of growth to the seventh. Aliquots (25 mL) were centrifuged at 5000× *g* for 5 min (Allegra X-30R, Beckman Coulter, Brea, IN, USA) to obtain the EC compounds. The supernatant was then filtered using a 0.45 µm Millipore® cellulose filter (Sartorius Stedim Biotech, Göttingen, Germany) to ensure cell removal. The pellet was resuspended and washed three times in 5 mL of Ringer's solution (38.5 µM NaCl, 1.41 µM KCl, 1.08 µM $CaCl_2$, 0.60 µM $NaHCO_3$) to obtain the IC compounds. A 5 mL sample of the resuspended cells was lysed with ultrasound (Ultrasonic Processor XL 2020, Misonix Inc., Connecticut, CT, USA) in three pulses of 10 s each at a fixed frequency of 20 kHz and 40% amplitude. The protein concentration of the IC and EC extracts was determined by Lowry's method at 541 nm [43] and calculated from a standard curve (0–20 mg mL^{-1}) using bovine serum albumin (Sigma Chemical Co., St. Louis, MI, USA) as standard.

2.5. Fluorescence Measurements

Excitation-emission matrices (EEM) and absorbance spectra were processed using an Aqualog® spectrofluorometer (Horiba Ltd., Kyoto, Japan). The EEM and absorbance spectra were recorded at 3 nm intervals in the excitation wavelength range of 240 to 600 nm in a 1 cm quartz cuvette. Emission spectra were also recorded every 3 nm. The fluorescence and absorption spectra were corrected by subtracting a high purity water sample (Raman water fluorescence reference, Starna®). Each EEM was corrected for inner filter effects using the Aqualog software. Fluorescence intensities were converted to Raman units (λex/λem 350/371–428 nm) [44] using the package 'staRdom' version 1.12 [45] for R version 3.6.1 [46].

Fluorescence signals in the EEMs were decomposed by PARAFAC using the 'drEEM' toolbox version 0.5 for MATLAB [47], using non-negativity constraints in all modes. A four-component model was validated, with a core consistency of 93.3 and an explained variance of 92.2%. No samples were excluded, for a total of 168 samples (12 species X 7 EC + 7 IC). Spectral loadings of the four PARAFAC components are given in Appendix A (Figure A1). The model was validated using split-half analysis [48] using a Tucker congruence coefficient of 0.95. The results of the half-split validation for the excitation and emission spectra of thee four components are given in Appendix A (Figure A2). The intensities of fluorescence of the four components are reported relative to the maximum intensity of each component.

2.6. Data Analysis

Bacterial abundance data were modeled using the exponential growth function $y = Co.\exp(-K \cdot t)$; *Co* is the initial concentration, and *K* the number of generations per unit of time.

Absorbance measurements for all samples (IC and EC) were converted to the Napierian absorption coefficients by $a(\lambda) = 2.303\, A(\lambda)/l$; where $A(\lambda)$ is the absorbance at wavelength λ, and "l" is the cuvette path length in meters. The absorption coefficient at 350 nm (*a*350) was taken as a proxy for dissolved organic carbon concentrations [49]. Spectral slope (S) of absorption coefficient [50] was calculated by fitting a Gaussian curve to the spectra using the equation: $y = a0 + e^{(-S(x-\lambda 0))} + K$. The spectral slope ratio (SR) [51] was calculated as the ratio of the slope from 275 to 295 nm ($S_{275–295}$) divided by the slope from 350 to 400 nm ($S_{350–400}$). The absorption ratio E2:E3 was calculated as the absorption at 250 nm divided by the absorption at 365 nm. The spectral slope (Sr) and ($S_{275–295}$) and ($S_{350–400}$) indicate relative molecular weight and aromaticity of CDOM [52]. The spectral slopes, E2:E3, and spectral slope ratios were calculated using the 'cdom' package for R [53].

We focus on five optical indices of CDOM: (i) the spectral absorption coefficient (aλ), which has been used as a proxy of dissolved carbon concentrations [54], (ii) the SR, which indicates relative differences in the average molecular weight (MW) of CDOM [51], (iii) the

biological index (BIX) [55] to determine the recent autochthonous contribution of CDOM, (iv) the fluorescence index (FI), which is a tracer of the origin of fluorescent CDOM [56], and (v) the humification index (HIX) for the humic content of the DOM [55]. These indices were calculated with the "eemR" package version 1.0.1 for *R* [57] (downloaded from https://github.com/PMassicotte/eemR, accessed on 20 January 2022). Packages 'eemR' and 'cdom' were run with R version 3.6.1 [46].

Canonical variant analysis (CVA) was used to identify the degree of discrimination between species according to the significant predictor variables. Redundancy analysis (RDA) was used to evaluate the statistical significance of the effect of the IC and EC compounds and species (explanatory variables) on the spectroscopic characteristics of dissolved organic matter (dependent variables). Prior to running the RDA analysis, all dependent variables were transformed to unit variance. RDA was performed under the stepwise regression modality using inclusion probabilities corrected by Bonferroni. A Monte Carlo permutation test with 9999 permutations was used to assess potential predictor variables [58]. All statistical analyzes were performed using XLSTAT (v2019.2, Addinsoft, NY, USA) and Canoco software v5.12.

3. Results

3.1. Phenotypic and Genotypic Identification of the Strains

Strain's identity was determined by sequence comparison in the NCBI-16S rRNA database (Table 1).

Table 1. Identification of heterotrophic bacterial species from seawater (SW) and freshwater (FW) based on information of the 16S ribosomal RNA gene.

Strain Code	Closest Phylogenetic Neighbor	NCBI:Txid	Source	Identity (%)
Baz	*Bacillus azotoformans*	1131731	SW	100
Bbd	*Bacillus badius*	1455	FW	99
Bcg	*Bacillus coagulans*	1398	FW	99
Bcq	*Bacillus macquariensis*	1468	FW	100
Bcr	*Bacillus cereus*	226900	SW	100
Blch	*Bacillus licheniformis*	279010	FW	98
Bmg	*Bacillus megaterium*	1348623	FW	100
Btoy	*Bacillus toyonensis*	121761	FW	100
Pal	*Paenibacillus alvei*	1206781	SW	99
Pis	*Psychrobacillus insolitus*	1461	FW	99
Ppy	*Paenibacillus polymyxa*	886882	FW	100
Ppy	*Paenibacillus polymyxa*	886882	SW	99

Nine species of *Bacillus* were identified, including *Psychrobacillus insolitus* and two species of *Paenibacillus*. The *P. polymyxa* species was isolated from both production systems (FW and SW). The results of the phenotypic characterization, including 22 biochemical tests, are shown in Table 2. Of the twelve strains identified, 45.5% showed the ability to use glucose as a carbon source, 36.4% used citrate, and 18.1% used both carbon sources.

Table 2. Phenotypic characterization of heterotrophic bacterial species.

Test Name	*B. macquariensis*	*B. badius*	*B. coagulans*	*B. licheniformis*	*P. insolitus*	*B. megaterium*	*B. cereus*	*P. alvei*	*P. polymyxa*	*P. toyonensis*	*B. azotoformans*
Gram	+	+	+	+	+	+	+	+	+	+	+
Oxidase	+	-	+		-	-	-	-	+		+
Catalase		+			+		+	+	+	+	-
Citrate			+	+			-	-	-	+	-
Swollen cell	+	-			-	-	+	-	-	-	-
Voges–Proskauer	-	-	+	+	-	-	+	-	+	+	-
β-galactosidase	-	-	-	-		-					
Lysine decarboxylase	-	+	-	-		-	+	-	+	+	+
Ornithine decarboxylase	+	+	-	-		-	+	+	-	-	+
Arginine decarboxylase	+	+	+	+		+	+	+	+	+	+
Amygdalin	-	-	-	-		+					
D-arabinose	-	-	+	-	+	+	-	-	-	-	-
Lactose	-	-	+	+	-	+					
Glucose	-	-	+	-	+	-	+	+	+	+	+
Inositol	-	-	-	-	-	+	-	-	-	-	-
Mannitol	-	-	-	+	-	-	-	-	-	-	-
Melibious	-	-	+	+			-	-	-	-	-
Rhamnose	-	-	-	-		+	-	-	-	-	-
Sorbitol	-	-	-	-		+	-	-	-	-	+
Urea	-	-	-	-	-	-	+	-	-	-	+
Starch	+	+	+	+	+	+	+	+	+	+	-
Growth in NaCl 6.5%	+	+	-	+	+	+	+	+	+	+	+

(+) = positive result to specific test, (-) = negative result to specific test.

3.2. Exponential Bacterial Growth

Figure 1 shows (a) exponential bacterial growth as a function of time and (b) total intracellular and extracellular protein concentration. The growth function, including the parameter *K*, is shown in Table 3. *P. alvei* and *B. badius* presented the highest generation time (0.0151 h and 0.0138 h, respectively). *B. toyonensis* had the slowest growth rate (0.0009 h), reaching $\log_{10}$ 8.07 cells mL^{-1} after 7 h.

Table 3. Exponential growth function of heterotrophic bacterial species; $\log_{10}$ y (cell mL^{-1}) = *Co*. exp $(-K \cdot t)$.

Bacteria	*Cf* (Cell mL^{-1})	*Co* (Cell mL^{-1})	*K*	R^2
B. azotoformans	8.196	8.013	0.0037	0.88
B. badious	8.573	7.892	0.0138	0.89
B. coagulans	8.066	8.253	0.0035	0.90
B. macquariensis	8.551	8.307	0.0048	0.96
B. cereus	8.295	7.817	0.0098	0.91
B. licheniformis	8.571	7.841	0.0066	0.90
B. megaterium	8.342	8.022	0.0065	0.85
B. toyonensis	8.066	8.019	0.0009	0.97
P. alvei	8.311	7.595	0.0151	0.98
P. insolitus	8.206	8.068	0.0028	0.90
P. polymyxa-FW	8.158	7.841	0.0065	0.89
P. polymyxa-SW	8.441	7.448	0.0213	0.90

Co = initial concentration, *Cf* = final concentration *K* = generation time.

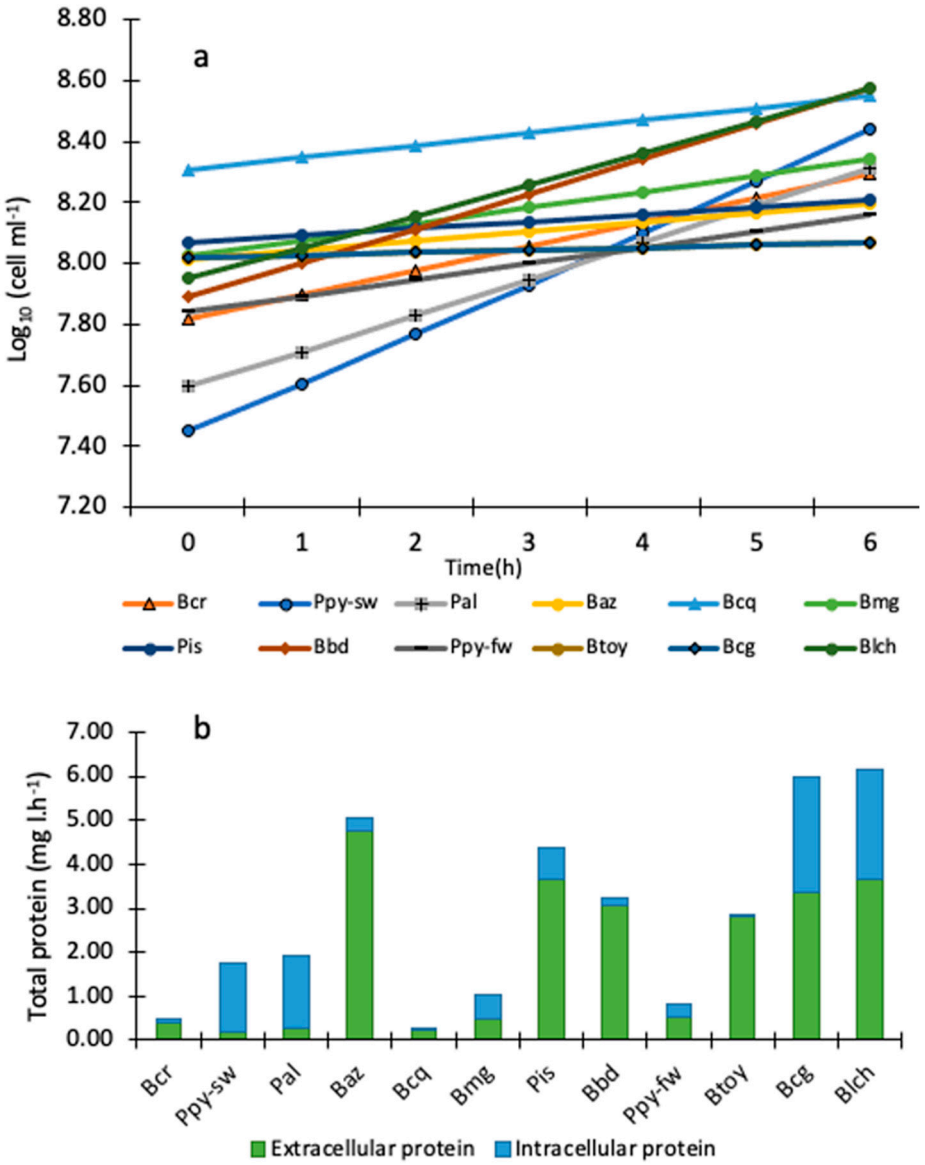

Figure 1. Exponential growth phase (**a**) and protein concentration (**b**) of heterotrophic bacterial species. Species key: Baz = *Bacillus azotoformans*, Bbd = *Bacillus badius*, Bcg = *Bacillus coagulans*, Bcq = *Bacillus macquariensis*, Bcr = *Bacillus cereus*, Blch = *Bacillus licheniformis*, Bmg = *Bacillus megaterium*, Btoy = *Bacillus toyonensis*, Pal = *Paenibacillus alvei*, Pis = *Psychrobacillus insolitus*, Ppy = *Paenibacillus polymyxa*-FW (freshwater); Ppy = *P. polymyxa*-SW (seawater).

In general, the EC protein concentration was higher than the IC in most bacteria, except for strains of the genus *Paenibacillus*. IC protein was 82% in *P. polymyxa*-SW and *P. alvei*. The EC protein reached 80% of *B. cereus*, *B. azotoformans*, *B. macquariensis*, *P. insolitus*, *B. badius*, and *B. toyonensis*. Species such as *B. megaterium*, *P. polymyxa*-fw, *B. coagulans*, and *B. licheniformis* showed a similar percentage of IC and EC protein (Figure 1b).

3.3. Fluorescence Characteristics and Identified Components

PARAFAC analysis indicated that the fluorescence signal can be mathematically decomposed into four independently varying fractions; the spectral loadings of all four components are shown in Appendix A. The results show two protein-type components (C1 and C4) and two humic-type components (C2 and C3). PARAFAC components obtained were compared to published spectra in the online OpenFluor database [59], and the results are shown in Table 4. Additionally, Cory and McKnight [60] interpret fluorescence in the

C2 region as their microbial oxidized Q3 peak, and our C3 as their SQ2 peak, suggesting the presence of oxidized and reduced quinones.

Table 4. Interpretation of the PARAFAC components in the OpenFluor spectral library.

Component	Interpretation	Reference
C1	Protein-like	Cawley et al., [61]
	Tryptophan-like, polyphenols	Yamashita et al., [62]
	Tryptophan-like, polyphenols	Yamashita et al., [63]
	Peak T, microbial	Hambly et al., [34]
C2	Terrestrial humic-like	Cawley et al., [61]
	Marine humic-like, peak M	Yamashita et al., [62]
	Humic-like	Yamashita et al., [63]
C3	Humic-like	Cohen et al., [64]
	Terrestrial humic/fulvic-like	Shakil et al., [65]
	Terrestrial humic-like	Lee et al., [66]
C4	Tryptophan and tyrosine-like	Cawley et al., [61]
	Peak T, tryptophan	Kowalczuk et al., [67]
	Protein-like	Murphy et al., [68]

C1 showed excitation/emission wavelengths of λ_{exc} = 275 nm/λ_{em} = 340 nm. This was associated with proteins containing tryptophan or Peak T, according to the designation by Coble [13]. C4 has excitation/emission wavelengths of λ_{exc} = 270 nm/λ_{em} = 310 nm and could not be classified using the peak definitions by Coble [18], but it was interpreted as a protein-like component in OpenFluor. C2 has excitation/emission wavelengths of λ_{exc} = 320 nm/λ_{em} = 410 nm and was associated with Coble's peaks C and M [18], terrestrial and marine humic-like compounds. C3 was detected at λ_{exc} = 240–244 nm/λ_{em} = 510–515 nm; this component was associated with Coble's peak A [18], which indicates that it is a substance similar to fulvic acid.

3.4. Biological Activity: Extracellular (EC) and Intracellular (IC) Bacterial Compounds

The forward selection of variables in RDA, using inclusion probabilities corrected by Bonferroni, showed that the cellular origin of the compounds (IC and EC, pseudo-F = 48.6; $p < 0.0001$) and the bacterial species (pseudo-F = 13.7; $p = 0.0001$) were significantly correlated with the spectroscopic characteristics of heterotrophic bacteria. The RDA using the first two canonical axes explained 40.56% of the total variance (Figure 2). The first axis (25.9% of total variance) explains the difference between the intracellular and extracellular components. The second canonical axis (8.3% of total variance) explains the difference between species, with *Bacillus macquariensis* at one end of the axis and *Bacillus coagulants* on the other end. Is interesting that differences between IC and EC components is larger than differences between bacterial species. Both axes are statistically significant (pseudo-F = 6.6; $p = 0.0001$, Monte Carlo test with 9999 permutations).

The fluorescence of C1 and C4 was 71.3% and 64.5% higher in the IC compounds than in the EC compounds. In contrast, C2 and C3 were 67.1% and 83.8% higher in EC compounds. The BIX was 54.1% higher in the IC compounds than in the EC ones, the opposite of HIX, which was 70.3% higher in the EC compounds. The absorption coefficient *a*350, the slope ratio (SR), the ratio of absorption coefficients (E2/E3), and $S_{275–295}$, $S_{350–400}$, were significantly higher in the EC compounds of all species. The fluorescence values and spectral data for each bacterium are shown in Tables 5 and 6. No fluorescence was detected in Ringer's medium, and no corrections were made to the sample EEMs.

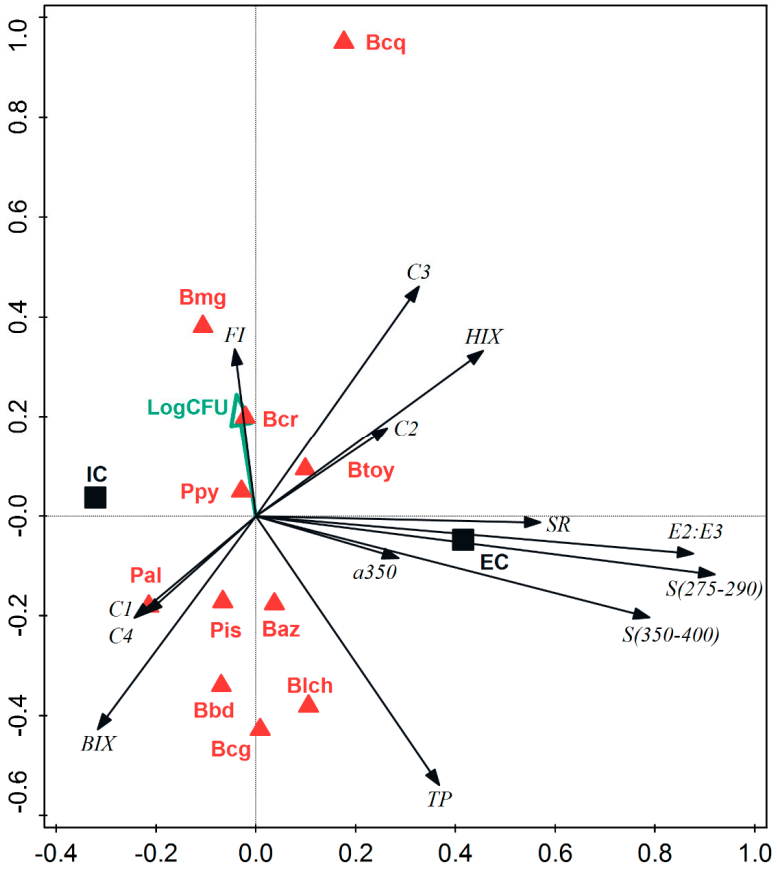

Figure 2. Redundancy analysis (RDA) showing the association between the response of the intracellular (IC) and extracellular (EC) compounds and bacterial species (independent variables) with PARAFAC components and absorbance spectral variables (response variables). Explained variance for axes 1 and 2 are shown in parentheses (pseudo-F = 6.6; p = 0.0001, Monte Carlo test with 9999 permutations). Species key: Baz = *Bacillus azotoformans*, Bbd = *Bacillus badius*, Bcg = *Bacillus coagulans*, Bcq = *Bacillus macquariensis*, Bcr = *Bacillus cereus*, Blch = *Bacillus licheniformis*, Bmg = *Bacillus megaterium*, Btoy = *Bacillus toyonensis*, Pal = *Paenibacillus alvei*, Pis = *Psychrobacillus insolitus*, Ppy = *Paenibacillus polymyxa* fw (freshwater); Ppy = *P. polymyxa* sw (seawater).

Table 5. Mean values of the PARAFAC components (Raman units ± S.E) and fluorescence indices of heterotrophic species after seven hours.

	C1	C2	C3	C4	FI	HIX	BIX
Extracellular compounds							
Baz	0.47 ± 0.10	0.52 ± 0.15	0.22 ± 0.06	0.39 ± 0.10	1.67 ± 0.03	1.32 ± 0.23	0.82 ± 0.01
Bbd	0.67 ± 0.15	0.49 ± 0.09	0.18 ± 0.05	2.79 ± 1.49	1.39 ± 0.03	0.78 ± 0.16	1.04 ± 0.02
Bcg	0.50 ± 0.05	0.51 ± 0.02	0.18 ± 0.01	0.88 ± 0.61	1.55 ± 0.02	1.21 ± 0.14	0.91 ± 0.01
Bcq	1.64 ± 0.36	0.33 ± 0.09	5.48 ± 1.15	0.49 ± 0.10	1.52 ± 0.01	3.50 ± 0.90	0.63 ± 0.09
Bcr	0.32 ± 0.05	0.29 ± 0.06	0.13 ± 0.03	0.14 ± 0.02	1.45 ± 0.05	1.06 ± 0.13	0.96 ± 0.03
Blch	0.29 ± 0.03	0.31 ± 0.05	0.19 ± 0.04	0.36 ± 0.13	1.30 ± 0.01	1.79 ± 0.17	0.79 ± 0.02
Bmg	4.37 ± 1.09	2.21 ± 0.48	2.49 ± 0.67	1.73 ± 0.44	1.45 ± 0.04	1.75 ± 0.33	0.91 ± 0.04
Btoy	0.37 ± 0.02	0.31 ± 0.03	0.14 ± 0.02	0.25 ± 0.05	1.40 ± 0.07	1.01 ± 0.10	0.94 ± 0.04
Pal	13.97 ± 4.26	0.28 ± 0.12	0.11 ± 0.04	3.54 ± 1.24	1.40 ± 0.05	1.53 ± 0.50	0.86 ± 0.06
Pis	0.63 ± 0.24	0.53 ± 0.27	0.28 ± 0.12	0.42 ± 0.20	1.39 ± 0.02	0.94 ± 0.10	0.95 ± 0.02
Ppy-fw	0.48 ± 0.06	0.46 ± 0.05	0.23 ± 0.04	0.37 ± 0.11	1.40 ± 0.06	1.13 ± 0.11	0.90 ± 0.01
Ppy-sw	0.40 ± 0.06	0.43 ± 0.07	0.28 ± 0.09	0.57 ± 0.21	1.35 ± 0.03	1.63 ± 0.15	1.00 ± 0.07

Table 5. *Cont.*

	C1	C2	C3	C4	FI	HIX	BIX
Intracellular compounds							
Baz	3.05 ± 0.81	0.17 ± 0.04	0.14 ± 0.03	2.18 ± 0.62	1.33 ± 0.02	0.30 ± 0.02	1.14 ± 0.07
Bbd	17.81 ± 8.20	0.26 ± 0.08	0.25 ± 0.05	5.91 ± 2.67	1.38 ± 0.07	0.60 ± 0.25	1.25 ± 0.11
Bcg	13.97 ± 4.26	0.17 ± 0.10	0.11 ± 0.04	3.54 ± 1.24	1.65 ± 0.07	0.13 ± 0.02	1.53 ± 0.11
Bcq	3.59 ± 1.43	0.83 ± 0.34	0.47 ± 0.14	1.79 ± 0.56	1.97 ± 0.16	1.75 ± 0.95	0.73 ± 0.11
Bcr	0.89 ± 0.24	0.28 ± 0.08	0.08 ± 0.01	0.42 ± 0.07	1.61 ± 0.10	0.89 ± 0.09	0.90 ± 0.11
Blch	4.71 ± 1.26	0.20 ± 0.02	0.10 ± 0.01	1.05 ± 0.29	1.62 ± 0.04	0.25 ± 0.05	1.39 ± 0.06
Bmg	1.80 ± 0.62	0.35 ± 0.11	0.19 ± 0.08	1.25 ± 0.31	1.65 ± 0.08	0.78 ± 0.08	0.87 ± 0.08
Btoy	1.27 ± 0.33	0.32 ± 0.10	0.20 ± 0.06	0.79 ± 0.18	1.84 ± 0.14	1.08 ± 0.33	0.75 ± 0.10
Pal	3.14 ± 1.61	0.12 ± 0.03	0.07 ± 0.02	1.12 ± 0.45	1.30 ± 0.10	0.42 ± 0.11	1.15 ± 0.19
Pis	2.77 ± 0.68	0.24 ± 0.07	0.09 ± 0.02	2.17 ± 0.54	1.16 ± 0.02	0.31 ± 0.01	1.07 ± 0.09
Ppy-fw	5.56 ± 1.58	0.18 ± 0.04	0.15 ± 0.02	1.30 ± 0.38	1.22 ± 0.23	0.94 ± 0.10	0.95 ± 0.02
Ppy-sw	1.71 ± 0.51	0.14 ± 0.03	0.06 ± 0.01	0.46 ± 0.11	1.41 ± 0.08	0.49 ± 0.15	1.16 ± 0.10

Species key: Baz = *Bacillus azotoformans*, Bbd = *Bacillus badius*, Bcg = *Bacillus coagulans*, Bcq = *Bacillus macquariensis*, Bcr = *Bacillus cereus*, Blch = *Bacillus licheniformis*, Bmg = *Bacillus megaterium*, Btoy = *Bacillus toyonensis*, Pal = *Paenibacillus alvei*, Pis = *Psychrobacillus insolitus*, Ppy = *Paenibacillus polymyxa*-FW (freshwater); Ppy = *P. polymyxa*-SW (seawater).

Table 6. Mean values (±S.E) of the spectral slope measurements of heterotrophic species after seven hours.

	a350	E2/E3	S275–295	S350–400	SR
Extracellular compounds					
Baz	52.47 ± 18.84	121.4 ± 19.66	0.75 ± 0.06	0.39 ± 0.07	40.89 ± 9.35
Bbd	182.66 ± 69.46	67.53 ± 11.90	0.57 ± 0.12	0.18 ± 0.06	99.54 ± 17.39
Bcg	34.67 ± 2.25	149.58 ± 6.55	0.80 ± 0.02	0.57 ± 0.02	34.43 ± 2.00
Bcq	51.17 ± 15.78	134.29 ± 26.06	0.63 ± 0.07	0.21 ± 0.05	72.33 ± 8.75
Bcr	24.90 ± 7.92	133.6 ± 14.49	0.77 ± 0.04	0.56 ± 0.05	22.45 ± 5.63
Blch	14.84 ± 3.15	202.35 ± 11.83	0.98 ± 0.16	0.77 ± 0.18	16.64 ± 3.57
Bmg	136.67 ± 85.94	138.99 ± 11.04	0.76 ± 0.04	0.33 ± 0.02	53.84 ± 3.43
Btoy	30.43 ± 5.42	145.29 ± 19.07	0.73 ± 0.03	0.62 ± 0.06	27.38 ± 1.30
Pal	47.77 ± 10.76	118.15 ± 13.27	0.63 ± 0.05	0.72 ± 0.04	42.38 ± 6.66
Pis	40.29 ± 4.97	153.77 ± 19.47	1.04 ± 0.06	0.15 ± 0.02	113.6 ± 0.01
Ppy-fw	153.23 ± 91.66	89.33 ± 14.69	0.59 ± 0.08	0.38 ± 0.08	50.88 ± 12.71
Ppy-sw	189.06 ± 96.47	63.91 ± 10.97	0.48 ± 0.09	0.21 ± 0.06	93.33 ± 32.45
Intracellular compounds					
Baz	21.27 ± 2.71	6.62 ± 0.73	0.06 ± 0.01	0.01 ± 0.00	17.26 ± 1.48
Bbd	55.17 ± 21.81	10.44 ± 2.88	0.06 ± 0.01	0.03 ± 0.02	9.86 ± 1.89
Bcg	29.43 ± 5.92	6.39 ± 0.08	0.04 ± 0.00	0.01 ± 0.00	8.27 ± 0.40
Bcq	13.17 ± 3.26	10.28 ± 1.25	0.07 ± 0.01	0.01 ± 0.00	10.44 ± 1.38
Bcr	5.40 ± 1.57	6.02 ± 0.62	0.05 ± 0.01	0.01 ± 0.00	11.15 ± 1.37
Blch	13.72 ± 3.53	7.40 ± 0.36	0.05 ± 0.00	0.01 ± 0.00	7.67 ± 0.36
Bmg	3.39 ± 0.53	11.70 ± 2.58	0.08 ± 0.01	0.02 ± 0.01	12.01 ± 1.64
Btoy	8.33 ± 1.82	15.50 ± 3.85	0.08 ± 0.01	0.02 ± 0.00	10.20 ± 1.33
Pal	14.65 ± 5.39	8.97 ± 1.09	0.07 ± 0.01	0.01 ± 0.00	13.45 ± 1.80
Pis	2.77 ± 0.68	0.24 ± 0.07	0.09 ± 0.02	2.17 ± 0.54	1.16 ± 0.02
Ppy-fw	22.76 ± 4.14	6.38 ± 0.53	0.04 ± 0.00	0.01 ± 0.00	10.80 ± 0.79
Ppy-sw	9.97 ± 2.25	5.86 ± 0.46	0.04 ± 0.00	0.02 ± 0.01	5.39 ± 0.98

Species key: Baz = *Bacillus azotoformans*, Bbd = *Bacillus badius*, Bcg = *Bacillus coagulans*, Bcq = *Bacillus macquariensis*, Bcr = *Bacillus cereus*, Blch = *Bacillus licheniformis*, Bmg = *Bacillus megaterium*, Btoy = *Bacillus toyonensis*, Pal = *Paenibacillus alvei*, Pis = *Psychrobacillus insolitus*, Ppy = *Paenibacillus polymyxa*-FW (freshwater); Ppy = *P. polymyxa*-SW (seawater).

3.5. Differences between Species

The differences between the bacterial groups, according to the significance of the spectral and fluorescence predictor variables of the CVA, are shown in Figure 3. The origin of the bacteria (FW, SW) was not a significant factor in the fluorescent or spectral variables of the analyzed species, so this factor was not considered in the analysis. The strains were divided into three groups with similar EC characteristics (Figure 3a). The PARAFAC C3 component and the spectral slope $S_{350–400}$ were the predictor variables that explained 86.6% of the difference between the groups (Table 7). *B. macquariensis* and *B. megaterium* were discriminated by their high C3 fluorescence (5.48 and 2.49 Raman units, respectively, Table 4). The spectral slope$S_{350–400}$ of *B. licheniformis* reached the highest value (0.77 nm), compared to *P. insolitus*, which showed the lowest EC value (0.15 nm; Table 5).

At the IC level, the FI, together with the value of BIX and SR, were the most significant predictors in the differentiation of species. Among them, they explained 78.4% of the inequality between the bacterial groups (Table 7). *B. macquariensis* once again stood out due to its higher IF value and the fluorescence of the C3 component (Figure 3b). The group formed by *B. coagulans*, *B. licheniformis*, *B. badius*, and *P. polymyxa*-sw were similar in their BIX value and *a*350. Bacteria such as *P. alvei*, *P. polymyxa*-fw, and *B. azotoformans* presented high SR value. *P. insolitus* had the lowest SR and the highest $S_{350–400}$ (Table 6).

Table 7. Discriminant variables of species selected from the canonical variant analysis (CVA) by stepwise forward regression.

Variables	R^2 Partial	F	Pr > F	Λ Wilks	Var (%)
Extracellular Fraction					
C3	0.759	15.998	<0.0001	0.241	65.78
$S_{350–400}$	0.684	10.813	<0.0001	0.076	20.80
E2/E3	0.641	8.759	<0.0001	0.027	7.47
C1	0.624	8.001	<0.0001	0.010	2.81
FI	0.497	4.670	<0.0001	0.005	1.41
$S_{275–295}$	0.420	3.354	0.002	0.003	0.82
C2	0.401	3.039	0.004	0.002	0.49
HIX	0.474	4.010	0.000	0.001	0.26
C4	0.389	2.782	0.007	0.001	0.16
SR	0.522	4.674	<0.0001	0.000	0.08
BIX	0.426	3.102	0.003	0.000	0.04
Intracellular Fraction					
FI	0.500	6.445	<0.0001	0.441	44.23
BIX	0.457	5.361	<0.0001	0.220	22.13
SR	0.378	3.813	0.000	0.120	12.01
*a*350	0.375	3.704	0.000	0.074	7.47
$S_{275–295}$	0.338	3.112	0.002	0.047	4.67
C3	0.294	2.504	0.011	0.031	3.09
HIX	0.266	2.140	0.029	0.022	2.18
$S_{350–400}$	0.256	1.998	0.043	0.016	1.60

TP = total protein concentration, FI = fluorescence index, BIX = biological index, SR = slope ratio, E2/E3 = a_{250}/a_{265}; C1, C2, C3, C4 = PARAFAC components.

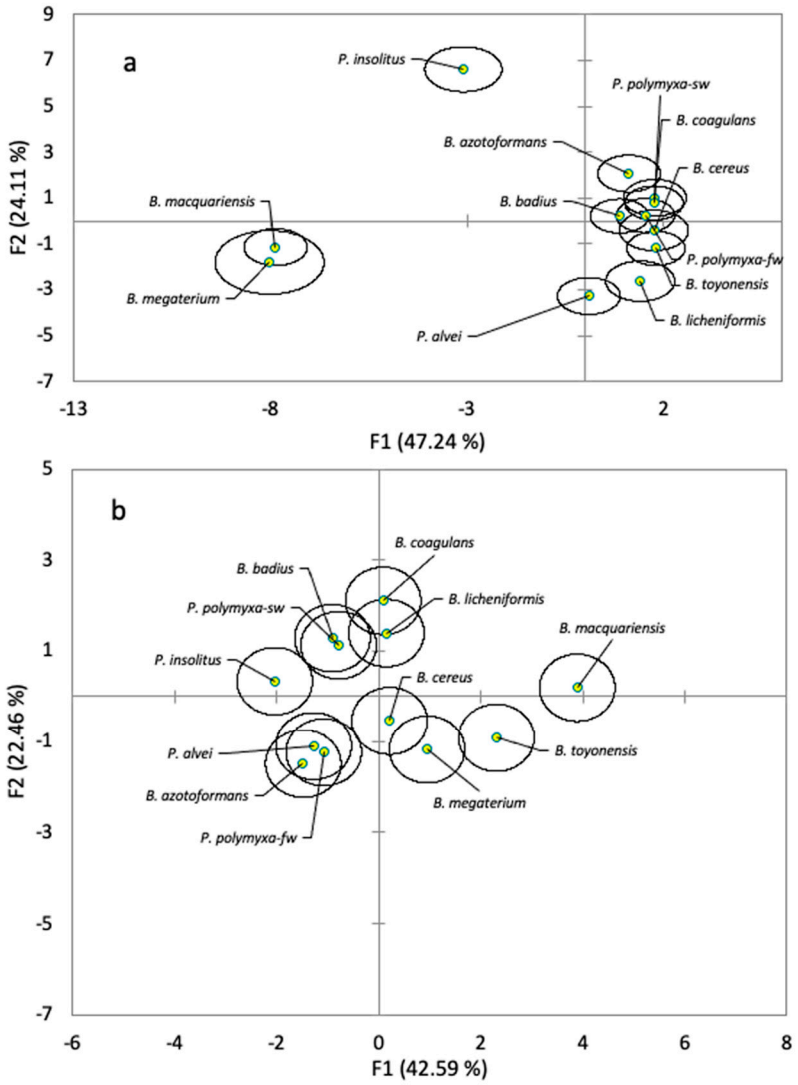

Figure 3. Canonical variant analysis (CVA) based on extracellular (**a**) and intracellular (**b**) PARAFAC components and absorbance spectral variables (response variables). Points represent the result of the CVA regression for each strain. Eigenvalues for axes 1 and 2 are shown in parentheses (p = <0.0001). Circles (centroids) = are the multivariate average for each group calculated from the discriminant functions. Species key: Baz = *Bacillus azotoformans*, Bbd = *Bacillus badius*, Bcg = *Bacillus coagulans*, Bcq = *Bacillus macquariensis*, Bcr = *Bacillus cereus*, Blch = *Bacillus licheniformis*, Bmg = *Bacillus megaterium*, Btoy = *Bacillus toyonensis*, Pal = *Paenibacillus alvei*, Pis = *Psychrobacillus insolitus*, Ppy = *Paenibacillus polymyxa* fw (freshwater); Ppy = *P. polymyxa* sw (seawater).

4. Discussion

The main finding of this work is the evidence of differential production of humic-type or protein-type FDOM production by HB species from marine and freshwater aquaculture systems in their intracellular and extracellular fractions, as well as CDOM with different relative molecular weights. Some bacteria, such as *B. azotoformans*, *B. coagulans*, and *B. licheniformis*, showed a high production of total protein per unit of time, although not necessarily associated with a fluorescent protein. Other species, such as *B. badius*, *B. macquariensis*, *B. megaterium*, and *P. alvei*, stood out for their high FDOM production at IC and EC levels. PARAFAC components C1 and C4 were associated with protein-like components and C2 and C3 with humic-like components. The highest percentage of C1 and C4 was present at the IC level, whereas the most significant amount of humic acid (C2 and C3) was present at the EC level. A similar finding was reported by Fox et al. [25] for other environmental microorganisms such as *Escherichia coli*, *Bacillus subtilis*, and *Pseudomonas*

aeruginosa. These authors revealed that the highest intensity of microbial fluorescence occurs in the IC space and may be associated with the presence of structural or functional biological molecules. Kallenbach et al. [69] reported that humic-type FDOM are molecules released extracellularly by bacterial cells, which agrees with our findings. In the present study, the main groups of organic fluorophores that showed fluorescence in HB are attributed to humic and fulvic acids (with blue fluorescence), as well as to the group of proteins (with UV fluorescence); this group consists of three dissolved fluorescent amino acids tryptophan, tyrosine, and phenylalanine. These findings suggest that some bacterial species are promising in providing essential amino acids for growing aquaculture organisms, and others have their main function as recyclers of organic matter.

B. macquariensis and *B. megaterium* release large amounts of extracellular humic-type FDOM, which was previously associated with the presence of polymeric molecules considered both chemically and biologically refractory [70]. In fact, the FI, which provides information on the source or degree of DOM degradation [71], was significantly higher in *B. macquariensis*, which makes this bacterium a candidate for in vitro culture and inoculation in heterotrophic aquaculture systems or even in biological biofilters to maintain water quality. *B. macquariensis* has been previously investigated for its high capacity to secrete extracellular xylanase, which is involved in the degradation of some components of the animal diet, such as cellulose [72,73]. This makes us think that this strain would be recycling part of the food not consumed by aquatic organisms.

B. megaterium synthesizes polymeric substances such as polyhydroxyalkanoates (PHA) that accumulate as cytoplasmic inclusions when they are grown on substrates rich in carbon sources [74]. Heterotrophic aquaculture production systems require the continuous addition of supplementary sources of carbohydrates in the water, which could stimulate the metabolism of PHA-producing species, explaining the high value of fluorescence. Other studies will be required to know the role of components C1 and C3 as possible indicators of the content of PHA present in aquaculture effluents.

The spectral and fluorescence EC characteristics between the microorganims were similar (63.3%). The main differences occurred at the IC level, mainly due to the contribution of two significant predictors, FI and BIX (<0.0001) (Figure 3b, Table 7). Bacteria such as *B. coagulans*, *B. licheniformes*, *B. badius*, and *P. alvei* stood out for their high value of intracellular BIX; these bacteria also generate a high concentration of cellular protein (Figure 1b). The BIX-CI close to 1 (1.05 ± 0.03) suggests recent and active CDOM production [56,75]. The high fluorescence of the C1 component in this group of microorganisms reflects the production of protein-like substances. These characteristics make them interesting candidates for the nutritional supplementation of omnivorous aquatic species. It is known that *B. badius* can colonize and remain in the intestine of tilapias cultured in biofloc at values ranging between 80 and 170 CFU/mL [76]. *B. licheniformis* produces enzymes that are released at the EC level, such as α-amylase (58.4 kDa) and alkaline proteases, called subtilisins (20–45 kDa) [77,78]. These enzymes could contribute to the enzymatic digestion process and favor the assimilation of food in cultured organisms. *P. alvei* was another interesting microorganism, which showed a high fluorescence of the C1 and C4 components, both of protein type. This microorganism produces flocculant polysaccharides composed of aminosugars and peptides with Gram (-) antimicrobial activity [79,80], which are possibly the origin of the fluorescence.

The extracellular spectral characteristics of *P. insolitus* differed from the rest of the bacteria (Figure 3). This strain showed an inverse relationship between $S_{275–295}$ and $S_{350–400}$ in the IC and EC fractions (Table 6), suggesting differences in the relative molecular weight or aromaticity [81] of these two fractions. For this species, the EC fraction has a higher $S_{275–295}$ than the $S_{350–400}$ value, with the opposite being true for the IC fraction. These characteristics mainly differentiated *P. insolitus* from bacteria such as *B. licheniformis* and *P. alvei*, both with high $S_{350–400}$ EC compared to the rest. The spectral slope values calculated for a small wavelength range for UVB (275–295 nm) and S values for UVB and UVA (350–400 nm) correlate negatively with molecular weight and photochemistry of exposure

to degradation [51,52,81]. This suggests that *P. insolitus* releases more low molecular weight extracellular molecules. The opposite occurs with *B. licheniformis* and *P. alvei*. There is not much information about the substances that *P. insolitus* can synthesize, which makes it difficult to understand their role in aquaculture systems. It is known that *P. alvei* eliminate the chlorophenol compounds that originate from lignin residues present in the food [82]. This function suggests that it would have an essential role in water bioremediation.

5. Conclusions

FDOM production varies between bacterial species, and this study provides evidence that freshwater and marine heterotrophic microbes can produce CDOM with different characteristics in their IC and EC fractions. The main groups of organic fluorophores that showed fluorescence at the extracellular level are attributed to humic and fulvic acids and at the intracellular level to the group of proteins represented by tryptophan, tyrosine, and phenylalanine. *B. badius* produced a high amount of protein-type FDOM; *B. macquariensis* and *B. megaterium* were shown to produce and release a high quantity of humic-type FDOM into the medium. *P. insolitus* presented unique spectral characteristics releasing low molecular weight extracellular molecules into the medium. For aquaculture, these findings suggest that some bacterial species are promising in providing essential amino acids for growing organisms, and others play their main role in the exchange of nutrients and the global carbon cycle.

Author Contributions: Conceptualization, M.G.-K. and G.G.-B.; methodology, M.G.-K., G.G.-B. and M.J.S.-S.; formal analysis, M.G.-K. and G.G.-B., writing—original draft preparation, M.G.-K. and G.G.-B.; writing—review and editing, M.G.-K., G.G.-B. and M.J.S.-S. All authors have read and agreed to the published version of the manuscript.

Funding: This work was supported by grants from the National Science and Technology Council (CONACYT, MX) (000009-01EXTV-00076).

Institutional Review Board Statement: Not applicable.

Informed Consent Statement: Not applicable.

Data Availability Statement: The data presented in this study are available on request from the corresponding author.

Acknowledgments: The authors wish to acknowledge the contributions of Stiene Beyens from Rhine-Waal University of Applied Science (Kleve, Germany), José G. García Gutierrez from Instituto Superior de Los Reyes (Michoacán, Mexico), M. Teresita Cantún Ruelas and Alejandra C. González Coello from University Marist of Merida (Mérida, Mexico) for their assistance in laboratory analysis and the field experiment. We are grateful to F. Espinosa Faller for his support for this research. Thank you to the two anonymous reviewers; their suggestions greatly improved our paper.

Conflicts of Interest: The authors declare no conflict of interest.

Appendix A

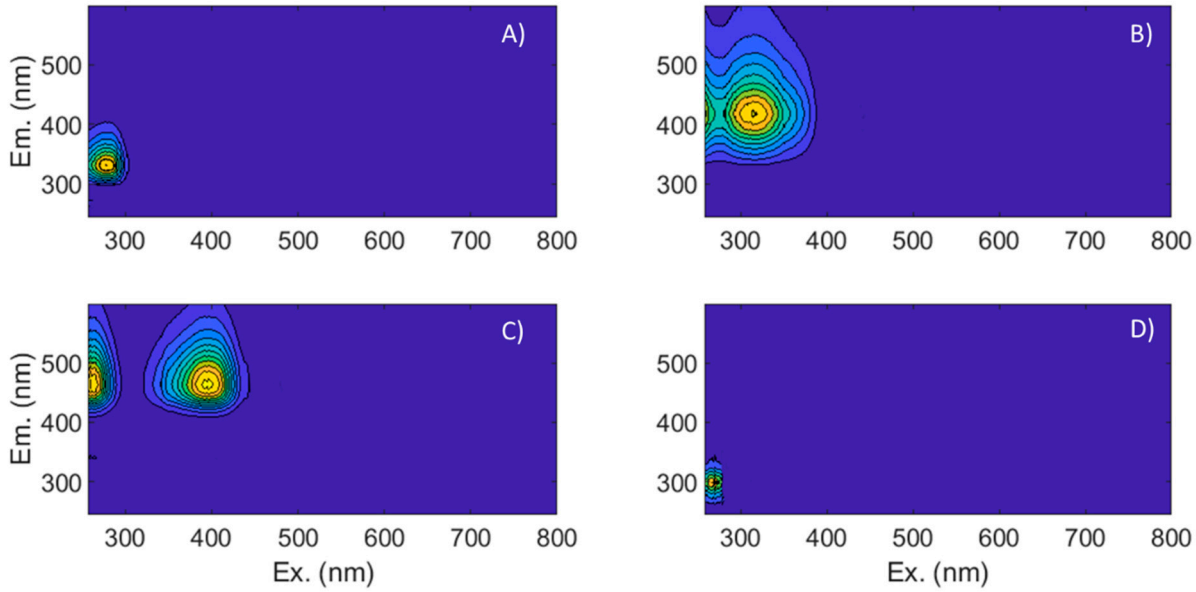

Figure A1. Excitation-emission matrices (EEMs) for the four PARAFAC components obtained in this study. (**A**) Component 1 (protein-like), (**B**) Component 2 (humic-like), (**C**) Component 3 (humic-like), and (**D**) Component 4 (protein-like).

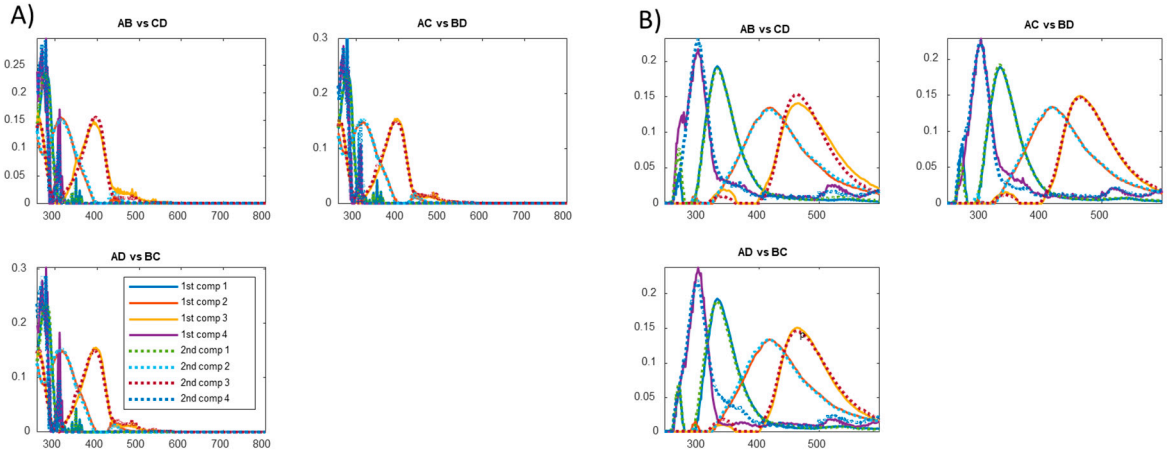

Figure A2. Half-split validation of the four PARAFAC components: (**A**) excitation spectra, and (**B**) emission spectra. All splits agree with a Tucker congruence coefficient higher than 0.95.

References

1. Buchan, A.; LeCleir, G.R.; Gulvik, C.A.; González, J.M. Master recyclers: Features and functions of bacteria associated with phytoplankton blooms. *Nat. Rev. Microbiol.* **2014**, *12*, 686–698. [CrossRef] [PubMed]
2. Carlson, C.A.; Giorgio, P.A.D.; Herndl, G.J. Microbes and the dissipation of energy and respiration: From cells to ecosystems. *Oceanography* **2007**, *20*, 89–100. [CrossRef]
3. Andrews, S.C.; Robinson, A.K.; Rodríguez-Quiñones, F. Bacterial iron homeostasis. *FEMS Microbiol. Rev.* **2003**, *27*, 215–237. [CrossRef]
4. Gram, L.; Grossart, H.P.; Schlingloff, A.; Kiorboe, T. Possible quorum sensing in marine snow bacteria: Production of acylated homoserine lactones by *Roseobacter* strains isolated from marine snow. *Appl. Environ. Microbiol.* **2002**, *68*, 4111–4116. [CrossRef] [PubMed]
5. Smith, D.C.; Simon, M.; Alldredge, A.L.; Azam, F. Intense hydrolytic enzyme-activity on marine aggregates and implications for rapid particle dissolution. *Nature* **1992**, *359*, 139–142. [CrossRef]
6. De Vos, P.; Garrity, G.; Jones, D.; Krieg, N.R.; Ludwig, W.; Rainey, F. Bergey's Manual of Systematic Bacteriology. In *The Firmicutes*; Springer Science & Business Media: Berlin, Germany, 2011; Volume 3.

7. Shimotori, K.; Watanabe, K.; Hama, T. Fluorescence characteristics of humic-like fluorescent dissolved organic matter produced by various taxa of marine bacteria. *Aquat. Microb. Ecol.* **2012**, *65*, 249–260. [CrossRef]
8. Noriega-Ortega, B.E.; Wienhausen, G.; Mentges, A.; Dittmar, T.; Simon, M.; Niggemann, J. Does the chemodiversity of bacterial exometabolomes sustain the chemodiversity of marine dissolved organic matter? *Front. Microbiol.* **2019**, *10*, 215. [CrossRef] [PubMed]
9. Guillemette, F.; del Giorgio, P.A. Simultaneous consumption, and production of fluorescent dissolved organic matter by lake bacterioplankton. *Environ. Microbiol.* **2012**, *14*, 1432–1443. [CrossRef]
10. Thompson, S.K.; Cotner, J.B. P-limitation drives changes in DOM production by aquatic bacteria. *Aquat. Microb. Ecol.* **2020**, *85*, 35–46. [CrossRef]
11. Avnimelech, Y. Carbon/nitrogen ratio as a control element in aquaculture systems. *Aquaculture* **1999**, *176*, 227–235. [CrossRef]
12. Milstein, A.; Avnimelech, Y.; Zoran, M.; Joseph, D. Growth performance of hybrid bass and hybrid tilapia in conventional and active suspension intensive ponds. *Isr. J. Aquac. Bamidgeh* **2001**, *53*, 147–157. [CrossRef]
13. Suárez-Puerto, B.; Delgadillo-Díaz, M.; Sánchez-Solís, M.J.; Gullian-Klanian, M. Analysis of the cost-effectiveness and growth of Nile tilapia (*Oreochromis niloticus*) in biofloc and green water technologies during two seasons. *Aquaculture* **2021**, *538*, 736534. [CrossRef]
14. De Schryver, P.; Crab, R.; Defoirdt, T.; Boon, N.; Verstraete, W. The basics of bio-flocs technology: The added value for aquaculture. *Aquaculture* **2008**, *277*, 125–137. [CrossRef]
15. Gullian Klanian, M.; Delgadillo Díaz, M.; Sánchez Solís, M.J.; Aranda, J.; Moreno Moral, P. Effect of the content of microbial proteins and the poly-β-hydroxybutyric acid in biofloc on the performance and health of Nile tilapia (*Oreochromis niloticus*) fingerlings fed on a protein-restricted diet. *Aquaculture* **2020**, *519*, 602–612. [CrossRef]
16. Attermeyer, K.; Hornick, T.; Kayler, Z.E.; Bahr, A.; Zwirnmann, E.; Grossart, H.-P.; Premke, K. Enhanced bacterial decomposition with increasing addition of autochthonous to allochthonous carbon without any effect on bacterial community composition. *Biogeosciences* **2014**, *11*, 1479–1489. [CrossRef]
17. Stedmon, C.A.; Markager, S.; Kaas, H. Optical properties and signatures of chromophoric dissolved organic matter (CDOM) in Danish coastal waters. *Estuar. Coast. Shelf Sci.* **2000**, *51*, 267–278. [CrossRef]
18. Coble, P.G. Characterization of marine and terrestrial DOM in seawater using excitation-emission matrix spectroscopy. *Mar. Chem.* **1996**, *51*, 325–346. [CrossRef]
19. Coble, P.G. Marine optical biogeochemistry: The chemistry of ocean color. *Chem. Rev.* **2007**, *107*, 402–418. [CrossRef]
20. Kramer, G.; Herndl, G. Photo and bioreactivity of chromophoric dissolved organic matter produced by marine bacterioplankton. *Aquat. Microb. Ecol.* **2004**, *36*, 239–246. [CrossRef]
21. Moran, M.A.; Sheldon, W.M.; Zepp, R.G. Carbon Loss and Optical Property Changes during Long-Term Photochemical and Biological Degradation of Estuarine Dissolved Organic Matter. *Limnol. Oceanogr.* **2010**, *45*, 1254–1264. [CrossRef]
22. Shimotori, K.; Omori, Y.; Hama, T. Bacterial production of marine humic-like fluorescent dissolved organic matter and its biogeochemical importance. *Aquat. Microb. Ecol.* **2010**, *58*, 55–66. [CrossRef]
23. Arai, K.; Wada, S.; Shimotori, K.; Omori, Y.; Hama, T. Production and degradation of fluorescent dissolved organic matter derived from bacteria. *J. Oceanogr.* **2018**, *74*, 39–52. [CrossRef]
24. Landa, M.; Blain, S.; Christaki, U.; Monchy, S.; Obernosterer, I. Shifts in bacterial community composition associated with increased carbon cycling in a mosaic of phytoplankton blooms. *ISMEJ* **2016**, *10*, 39–50. [CrossRef] [PubMed]
25. Fox, B.G.; Thorn, R.M.S.; Anesio, A.M.; Reynolds, D.M. The in situ bacterial production of fluorescent organic matter; an investigation at a species level. *Water Res.* **2017**, *125*, 350–359. [CrossRef]
26. Ni, B.J.; Fang, F.; Xie, W.M.; Sun, M.; Sheng, G.P.; Li, W.H.; Yu, H.Q. Characterization of extracellular polymeric substances produced by mixed microorganisms in activated sludge with gel-permeating chromatography, excitation-emission matrix fluorescence spectroscopy measurement and kinetic modeling. *Water Res.* **2009**, *43*, 1350–1358. [CrossRef]
27. Miao, L.; Zhang, Q.; Wang, S.; Li, B.; Wang, Z.; Zhang, S.; Zhang, M.; Peng, Y. Characterization of EPS compositions and microbial community in an Anammox SBBR system treating landfill leachate. *Bioresour. Technol.* **2018**, *249*, 108–116. [CrossRef]
28. Bai, Y.; Su, R.; Yao, Q.; Zhang, C.; Shi, X. Characterization of chromophoric dissolved organic matter (CDOM) in the Bohai Sea and the Yellow Sea using Excitation-Emission Matrix Spectroscopy (EEMs) and Parallel Factor Analysis (PARAFAC). *Estuaries Coasts.* **2017**, *40*, 1325–1345. [CrossRef]
29. Hou, X.; Liu, S.; Feng, Y. The autofluorescence characteristics of bacterial intracellular and extracellular substances during the operation of anammox reactor. *Sci. Rep.* **2017**, *7*, 39289. [CrossRef]
30. Parlanti, E.; Wörz, K.; Geoffroy, L.; Lamotte, M. Dissolved organic matter fluorescence spectroscopy as a tool to estimate biological activity in a coastal zone submitted to anthropogenic inputs. *Org. Geochem.* **2000**, *31*, 1765–1781. [CrossRef]
31. Hudson, N.; Baker, A.; Reynolds, D. Fluorescence analysis of dissolved organic matter in natural, waste and polluted waters—A review. *River Res. Appl.* **2007**, *23*, 631–649. [CrossRef]
32. Murphy, K.R.; Stedmon, C.A.; Waite, T.D.; Ruiz, G.M. Distinguishing between terrestrial and autochthonous organic matter sources in marine environments using fluorescence spectroscopy. *Mar. Chem.* **2008**, *108*, 40–58. [CrossRef]
33. Stedmon, C.A.; Bro, R. Characterizing dissolved organic matter fluorescence with parallel factor analysis: A tutorial. *Limnol. Oceanogr. Methods* **2008**, *6*, 572–579. [CrossRef]

34. Hambly, A.C.; Arvin, E.; Pedersen, L.F.; Pedersen, P.B.; Seredyńska-Sobecka, B.; Stedmon, C.A. Characterising organic matter in recirculating aquaculture systems with fluorescence EEM spectroscopy. *Water Res.* **2015**, *83*, 112–120. [CrossRef] [PubMed]
35. Gullian-Klanian, M.; Gold-Bouchot, G.; Delgadillo-Díaz, M.; Aranda, J.; Sánchez-Solís, M.J. Effect of the use of *Bacillus* spp. on the characteristics of dissolved fluorescent organic matter and the phytochemical quality of *Stevia rebaudiana* grown in a recirculating aquaponic system. *Environ. Sci. Pollut. Res.* **2021**, *28*, 26326–36343. [CrossRef] [PubMed]
36. Goto, S.; Tada, Y.; Suzuki, K.; Yamashita, Y. Production and reutilization of fluorescent dissolved organic matter by a marine bacterial strain, *Alteromonas macleodii*. *Front. Microbiol.* **2017**, *8*, 507. [CrossRef] [PubMed]
37. Goto, S.; Tada, Y.; Suzuki, K.; Yamashita, Y. Evaluation of the production of dissolved organic matter by three marine bacterial strains. *Front. Microbiol.* **2020**, *11*, 584419. [CrossRef] [PubMed]
38. Logan, N.A.; De Vos, P. Bacillus. In *Bergey's Manual of Systematics of Archaea and Bacteria*; John Wiley & Sons, Ltd.: Chichester, UK, 2015; pp. 1–163.
39. Altschul, S.F.; Gish, W.; Miller, W.; Myers, E.W.; Lipman, D.J. Basical Local Alignment Search Tool (BLAST). *J. Mol. Biol.* **1990**, *215*, 403–410. [CrossRef]
40. Lane, D. 16S/23S rRNA Sequencing. In *Nucleic Acid Techniques in Bacterial Systematics*; Stackebrandt, E., Goodfellow, M., Eds.; Wiley: New York, NY, USA, 1991; pp. 115–175.
41. Liu, L.; Ji, M.; Wang, F.; Wang, S.; Qin, G. Insight into the influence of microbial aggregate types on nitrogen removal performance and microbial community in the anammox process—A review and meta-analysis. *Sci. Total Environ.* **2020**, *714*, 136571. [CrossRef]
42. Ranganayaki, S.; Mohan, C. Effect of Sodium molybdate on microbial fixation of nitrogen. *Zeitschrift für Allgemeine Mikrobiologie* **1981**, *21*, 607–610. [CrossRef] [PubMed]
43. Lowry, O.H.; Rosebrough, N.J.; Farr, A.L.; Randall, R.J. Protein measurement with the Folin phenol reagent. *J. Biol. Chem.* **1951**, *193*, 265–275. [CrossRef] [PubMed]
44. Lawaetz, A.J.; Stedmon, C.A. Fluorescence Intensity Calibration Using the Raman Scatter Peak of Water. *Appl. Spectrosc.* **2009**, *63*, 936–940. [CrossRef] [PubMed]
45. Pucher, M.; Wünsch, U.; Weigelhofer, G.; Murphy, K.; Hein, T.; Graeber, D. staRdom: Versatile Software for analyzing spectroscopic data of dissolved organic matter in R. *Water* **2019**, *11*, 2366. [CrossRef]
46. R Development Core Team. *R: A Language and Environment for Statistical Computing*; R Foundation for Statistical Computing: Vienna, Austria, 2019.
47. Murphy, K.R.; Stedmon, C.A.; Graeber, D.; Bro, R. Fluorescence spectroscopy and multi-way techniques. PARAFAC. *Anal. Methods* **2013**, *5*, 6557–6566. [CrossRef]
48. Stedmon, C.A.; Markager, S. Tracing the production and degradation of autochthonous fractions of dissolved organic matter by fluorescence analysis. *Limnol Oceanog.* **2005**, *50*, 1415–1426. [CrossRef]
49. Massicotte, P.; Asmala, E.; Stedmon, C.; Markager, S. Global distribution of dissolved organic matter along the aquatic continuum: Across rivers, lakes and oceans. *Sci. Total Environ.* **2017**, *609*, 180–191. [CrossRef]
50. Loiselle, S.A.; Bracchini, L.; Cózar, A.; Dattilo, A.M.; Tognazzi, A.; Rossi, C. Variability in photobleaching yields and their related impacts on optical conditions in subtropical lakes. *J. Photochem. Photobiol. B Biol.* **2009**, *95*, 129–137. [CrossRef]
51. Helms, J.; Stubbins, A.; Ritchie, J.D.; Minor, E.C.; Kieber, D.J.; Mopper, K. Absorption spectral slopes and slope ratios as indicators of molecular weight, source, and photobleaching of chromophoric dissolved organic matter. *Limnol. Oceanogr.* **2009**, *53*, 955–969. [CrossRef]
52. Li, P.; Jin, H. Utilization of UV-Vis Spectroscopy and Related Data Analyses for Dissolved Organic Matter (DOM) Studies: A Review. *Crit. Rev. Environ. Sci. Technol.* **2017**, *47*, 131–154. [CrossRef]
53. Massicotte, P.; Markager, S. Using a Gaussian decomposition approach to model absorption spectra of chromophoric dissolved organic matter. *Mar. Chem.* **2016**, *180*, 24–32. [CrossRef]
54. Del Vecchio, R.; Blough, N.V. Photobleaching of chromophoric dissolved organic matter in natural waters: Kinetics and modeling. *Mar. Chem.* **2002**, *78*, 231–253. [CrossRef]
55. Huguet, A.; Vacher, L.; Relexans, S.; Saubusse, S.; Froidefond, J.M.; Parlanti, E. Properties of fluorescent dissolved organic matter in the Gironde Estuary. *Org. Geochem.* **2009**, *40*, 706–719. [CrossRef]
56. McKnight, D.M.; Boyer, E.W.; Westerhoff, P.K.; Doran, P.T.; Kulbe, T.; Andersen, D.T. Spectrofluorometric characterization of dissolved organic matter for indication of precursor organic material and aromaticity. *Limnol. Oceanogr.* **2001**, *46*, 38–48. [CrossRef]
57. Massicotte, P. GitHube.com. Cánada. 2019. Available online: www.pmassicotte.com/eemr/ (accessed on 12 December 2021).
58. ter Braak, C.J.F. Canonical community ordination. Part I: Basic theory and linear methods. *Ecoscience* **1994**, *1*, 127–140. [CrossRef]
59. Murphy, K.R.; Stedmon, C.A.; Wenig, P.; Bro, R. OpenFluor- An online spectral library of auto-fluorescence by organic compounds in the environment. *Anal. Methods* **2014**, *6*, 658–661. [CrossRef]
60. Cory, R.M.; McKnight, D.M. Fluorescence Spectroscopy Reveals Ubiquitous Presence of Oxidized and Reduced Quinones in Dissolved Organic Matter. *Environ. Sci. Technol.* **2005**, *39*, 8142–8149. [CrossRef]
61. Cawley, K.M.; Ding, Y.; Fourqurean, J.; Jaffé, R. Characterising the sources and fate of dissolved organic matter in Shark Bay, Australia: A preliminary study using optical properties and stable carbon isotopes. *Mar. Freshw. Res.* **2012**, *63*, 1098–1107. [CrossRef]
62. Yamashita, Y.; Maie, N.; Briceño, H.; Jaffé, R. Optical characterization of dissolved organic matter in tropical rivers of the Guayana Shield, Venezuela. *J. Geophys. Res. Biogeosci.* **2010**, *115*, G1. [CrossRef]

63. Yamashita, Y.; Panton, A.; Mahaffey, C.; Jaffé, R. Assessing the spatial and temporal variability of dissolved organic matter in Liverpool Bay using excitation-emission matrix fluorescence and parallel factor analysis. *Ocean. Dyn.* **2011**, *61*, 569–579. [CrossRef]
64. Cohen, E.; Levy, G.J.; Borisover, M. Fluorescent components of organic matter in wastewater: Efficacy and selectivity of the water treatment. *Water Res.* **2014**, *55*, 323–334. [CrossRef]
65. Shakil, S.; Tank, S.E.; Kokelj, S.V.; Vonk, J.E.; Zolkos, S. Particulate dominance of organic carbon mobilization from thaw slumps on the Peel Plateau, NT: Quantification and implications for stream systems and permafrost carbon release. *Environ. Res. Lett.* **2020**, *15*, 114019. [CrossRef]
66. Lee, S.A.; Kim, T.H.; Kim, G. Tracing terrestrial versus marine sources of dissolved organic carbon in a coastal bay using stable carbon isotopes. *Biogeosciences* **2020**, *17*, 135–144. [CrossRef]
67. Kowalczuk, P.; Tilstone, G.H.; Zabłocka, M.; Röttgers, R.; Thomas, R. Composition of dissolved organic matter along an Atlantic Meridional Transect from fluorescence spectroscopy and Parallel Factor Analysis. *Mar. Chem.* **2013**, *157*, 170–184. [CrossRef]
68. Murphy, K.R.; Ruiz, G.M.; Dunsmuir, W.T.M.; Waite, T.D. Optimized Parameters for Fluorescence-Based Verification of Ballast Water Exchange by Ships. *Environ. Sci. Technol.* **2006**, *40*, 2357–2362. [CrossRef]
69. Kallenbach, C.M.; Frey, S.D.; Grandy, A.S. Direct evidence for microbial-derived soil organic matter formation and its ecophysiological controls. *Nat. Commun.* **2016**, *7*, 13630. [CrossRef] [PubMed]
70. Findlay, S.E.; Sinsabaugh, R.L.; Sobczak, W.V.; Hoostal, M. Metabolic and structural response of hyporheic microbial communities to variations in supply of dissolved organic matter. *Limnol. Oceanogr.* **2003**, *48*, 1608–1617. [CrossRef]
71. Fellman, J.B.; Hood, E.; Spencer, R.G. Fluorescence spectroscopy opens new windows into dissolved organic matter dynamics in freshwater ecosystems: A review. *Limnol. Oceanogr.* **2010**, *55*, 2452–2462. [CrossRef]
72. Hoshino, T.; Takehashi, S.; Fujiwara, M.; Kasuya, T. *Typhula maritima*, a new species of Typhula collected from coastal dunes in Hokkaido, northern Japan. *Mycoscience* **2009**, *50*, 430–437. [CrossRef]
73. Sharma, M.; Kumar, A. Optimization of xylanase secretion from *Paenibacillus macquariensis*. *Curr. Trends Biotechnol. Pharm.* **2012**, *6*, 190–195.
74. Reddy, C.S.K.; Ghai, R.; Kalia, V.C. Polyhydroxyalkanoates: An overview. *Bioresour. Technol.* **2003**, *87*, 137–146. [CrossRef]
75. Hansen, A.M.; Kraus, T.E.C.; Pellerin, B.A.; Fleck, J.A.; Downing, B.D.; Bergamaschi, D.A. Optical properties of dissolved organic matter (DOM): Effects of biological and photolytic degradation. *Limnol. Oceanogr.* **2016**, *61*, 1015–1032. [CrossRef]
76. Pérez-Fuentes, J.A.; Pérez-Rostro, C.I.; Hernández-Vergara, M.P.; Monroy-Dosta, M.D.C. Variation of the bacterial composition of biofloc and the intestine of Nile tilapia *Oreochromis niloticus*, cultivated using biofloc technology, supplied different feed rations. *Aquac. Res.* **2018**, *49*, 3658–3668. [CrossRef]
77. Veith, B.; Herzberg, C.; Steckel, S.; Feesche, J.; Maurer, K.H.; Ehrenreich, P.; Bäumer, S.; Henne, A.; Liesegang, H.; Merkl, R.; et al. The complete genome sequence of *Bacillus licheniformis* DSM13, an organism with great industrial potential. *Microb. Physiol.* **2004**, *7*, 204–211. [CrossRef] [PubMed]
78. Rey, M.W.; Ramaiya, P.; Nelson, B.A.; Brody-Karpin, S.D.; Zaretsky, E.J.; Tang, M.; de Leon, A.L.; Xiang, H.; Gusti, V.; Clausen, I.G.; et al. Complete genome sequence of the industrial bacterium *Bacillus licheniformis* and comparisons with closely related Bacillus species. *Genome Biol.* **2004**, *5*, r77. [CrossRef] [PubMed]
79. Anandaraj, B.; Vellaichamy, A.; Kachman, M.; Selvamanikandan, A.; Pegu, S.; Murugan, V. Co-production of two new peptide antibiotics by a bacterial isolate *Paenibacillus alvei* NP75. *Biochem. Biophys. Res. Commun.* **2009**, *379*, 179–185. [CrossRef] [PubMed]
80. Abdel-Aziz, S.M.; Hamed, H.A.; Mouafi, F.E.; Abdelwahed, N.A. Extracellular metabolites produced by a novel strain, *Bacillus alvei* NRC-14: 3. Synthesis of a bioflocculant that has chitosan-like structure. *Life Sci. J.* **2011**, *8*, 883–890. [CrossRef]
81. Guéguen, C.; Cuss, C.W. Characterization of aquatic dissolved organic matter by asymmetrical flow field-flow fractionation coupled to UV–Visible diode array and excitation emission matrix fluorescence. *J. Chromatog. A* **2011**, *1218*, 4188–4198. [CrossRef] [PubMed]
82. Wang, C.C.; Lee, C.M.; Kuan, C.H. Removal of 2, 4-dichlorophenol by suspended and immobilized *Bacillus insolitus*. *Chemosphere* **2000**, *41*, 447–452. [CrossRef]